communications biology

Article

https://doi.org/10.1038/s42003-024-07194-2

3D keloid spheroid model: Development and application for personalized drug response prediction

YoungHwan Choi[1,2], Hyung-Suk Jang[1], Joonho Shim[1], Eunhye Yeo[1,2], Min-Hee Kim[1], Hyungrye Noh[1], Sejin Oh[1], Ji-Hye Park[1], Dongyoun Lee[1] & Jong Hee Lee[1,2]

Research on keloid is limited by the lack of proper in vitro and animal model reflecting in vivo status. Based on heterogeneity of keloid and important role of endothelial cells in its pathogenesis, a novel 3D in vitro keloid spheroid prepared with keloid fibroblasts and endothelial cells was evaluated in this study. Commercial cell lines of keloid fibroblasts and endothelial cells were used at various cellular ratios to generate keloid spheroids to determine the optimal condition. Keloid spheroids from three keloid patients were also made and their usefulness as in vitro models, including their responses to drugs, were assessed. Spheroids with higher endothelial cell proportions exhibited increased viability and propagation ability. Patient-derived keloid spheroids showed heterogeneity which might reflect individual clinical conditions. The optimal ratio of fibroblasts to endothelial cells was determined to be 4:1 for keloid spheroids based on gene expression and viability analyses. Patient-derived keloid spheroid showed better keloidal changes in genetic expressions than 2D monolayer culture. Spheroids exhibited varied responses and resistance to each drug used for keloids, depending on the cell type used. 3D keloid spheroids might provide an effective in vitro model for investigating disease pathogenesis and appropriate treatment modalities for future precision medicine.

Keloid is a non-cancerous fibroproliferative disorder that develops beyond the margins of an initial wound. It shows an excessive thickened collagen deposition in the dermis with a high vascularity. Although various treatments, including intralesional injections of triamcinolone, fluorouracil, and bleomycin, have been tried for keloids, treatment responses vary among patients and lesions. Currently, there is no way to predict drug response before treatment.

Since keloid is a unique disease of humans, it is hard to make an animal model. Diverse in vitro keloid models have been reported[1–3]. Of them, the most commonly used in vitro keloid model is a two-dimensional (2D) monolayer fibroblast cell culture system. However, it has a fundamental limitation of having little cellular interactions and collagen depositions, which are major characteristics of keloids[3,4]. Although co-culture models show increased cellular interactions to some degree, they cannot reflect tissue architecture[3].

The three-dimensional (3D) cultural technique is widely used to study the pathogenesis of diverse tumorous conditions, especially cancers[5]. Among currently available 3D culture models, organoids might reflect the in vivo environment better than spheroids. However, they have lower productivity and longer generating time than spheroids[3]. Spheroids can be generated massively with a short generation time. In addition, they reflect both cellular interactions and tissue architecture[5–7]. Previous studies have demonstrated that spheroids are 3D cell culture models with increased cellular interactions, resembling genetic expression profiles of in vivo tissues[8,9]. The potential use of spheroid models for drug screening and optimization has been evaluated in multiple studies[6,10].

However, spheroids have not been widely used for studying keloids so far. Previously reported keloid spheroids simply used harvested keloid tissues themselves from the central dermal layer of an active stage keloid patient without epidermis. Authors have cultured primary keloid spheroid under submerged conditions[11]. In addition, since a 2D monolayer cell culture of keloid fibroblasts shows limited genetic expression profiles associated with fibrosis, spheroids in keloid studies are thought to be helpful for modeling keloids[12].

Heterotypic cellular interaction is an important factor in the pathogenesis of keloids. Previous studies have mainly focused on cellular

[1]Department of Dermatology, Samsung Medical Center, Sungkyunkwan University School of Medicine, Seoul, Republic of Korea. [2]Department of Medical Device Management and Research, Samsung Advanced Institute for Health Sciences and Technology, Sungkyunkwan University, Seoul, Republic of Korea.
e-mail: bell711@hanmail.net

interactions of keratinocytes and fibroblasts in keloids so far[13,14]. However, endothelial dysfunction is thought to play an important role in the pathogenesis of keloids recently[15]. Recent advances in single-cell RNA sequencing technologies have also revealed that endothelial cells play a critical role in the pathogenesis of keloids[16,17]. In our previous study on keloids using single-cell RNA sequencing and spatial transcriptomics, we observed that the expression of keloid marker genes was elevated in the deep dermis surrounding blood vessels, but not in the superficial dermis[16]. This finding led us to focus on the importance of endothelial cells rather than keratinocytes in keloids and to develop the idea of a spheroid model to examine the interactions between fibroblasts and endothelial cells. In previous studies where fibroblasts were used to create spheroids, deactivation of fibroblasts was observed[18,19]. However, these studies only utilized fibroblasts to form the spheroids. Our research aims to investigate the effects when spheroids are composed of a mixture of fibroblasts and endothelial cells. By examining the interactions between endothelial cells and fibroblasts, which are crucial to the pathophysiology of keloids, we aim to develop a more representative model of keloids.

In this study, due to the absence of suitable in vivo and animal models for keloids, we propose the development of a 3D structured model. Initially, we utilized spheroid technology to establish a more precise in vitro model of keloids, incorporating keloid fibroblasts and endothelial cells. Subsequent steps involved evaluating the biological activities, gene expression profiles, and drug responses of these keloid spheroids. This comprehensive evaluation aimed to validate the spheroid model's utility as a reliable tool for studying keloids and assessing drug efficacy. The primary goal is to develop personalized treatment strategies where drug responses observed in patient-derived models can guide the optimization of therapeutic regimens for individual patients.

Results

Formation of keloid spheroids using ATCC keloid fibroblasts and endothelial cells

First of all, a commercial cell line (CRL1762, ATCC, Manassas, VA, USA) of keloid fibroblasts was used to determine the optimal condition of keloid spheroids. Keloid spheroids were formed using ATCC keloid fibroblasts (F) and HUVECs (E) at ratios of 1:0 (A(F1E0)), 8:1 (A(F8E1)), 4:1 (A(F4E1)), 2:1 (A(F2E1)), and 1:1 (A(F1E1)). We found that aggregated cells changed their densities. Therefore, we classified them into different states such as aggregate, pre-compaction, compact spheroid, pre-regression, and regression (Fig. 1a). According to cellular ratio, keloid spheroids showed different state changes (Fig. 1b, c). In A(F1E0), compact spheroids were formed on day 2, which was the earliest. However, they could not maintain compactness, eventually regressing after day 4. On the other hand, compact spheroids started to form on day 3 and plateaued from day 4 to day 6 in A(F8E1), A(F4E1), and A(F2E1). Since A(F1E1) could not form a compact spheroid until day 6, the 1:1 ratio was thought to be an inadequate ratio for further analysis. Taken together, endothelial cells were thought to be needed for maintaining keloid spheroids. However, too many endothelial cells disrupted the formation of keloid spheroids. In addition, it was found that at least 4 days were needed to form and maintain compact spheroids in keloid.

Next, we measured areas of spheroids and set the area of A(F1E0) as a control (Fig. 1d). At day 6, the area of the spheroid ranged from 10,804 to 25,118 μm^2. The area was the largest for A(F1E1) and the second largest for A(F4E1), both showing a significant increase compared to the area of A(F1E0). However, A(F1E1) could not form compact spheroids as mentioned above. A(F4E1) could form and maintain compact spheroids with a large area.

Cell viability assay of keloid spheroids

Results of cell viability assay showed that A(F1E0) had a low cell viability in the center from day 4 (Fig. 2). On the contrary, spheroids with endothelial cells had higher cell viability in the center. Cell viability was likely to be increased with a higher proportion of endothelial cells. When comparing keloid spheroids on day 6 with those on day 4, the size of the spheroids decreased across all groups, which suggests that nonviable cells in 3D spheroids gradually detached between day 4 and day 6.

Composition and propagation assay of keloid spheroids

Since compact spheroids were maintained from day 4 while nonviable cells were increased after day 4, we used day 4 spheroids to perform the following analyses. We determined cellular composition with confocal fluorescence microscopy and propagation ability with propagation assay (Fig. 3). Results of the composition assay using confocal microscopy confirmed that fibroblasts and endothelial cells were well mixed in all groups (Fig. 3a). Next, we examined and quantified propagation area of keloid spheroids by performing a propagation assay (Fig. 3b, c). Since both the sprouting area of endothelial cells and the proliferating area of fibroblasts could be present in the propagation area, we set the propagation area of A(F1E0) as a control. A(F4E1) and A(F2E1) showed significantly increased propagation areas compared to A(F1E0) at day 5. Therefore, A(F4E1) and A(F2E1) showed higher propagation abilities than other spheroids.

Determination of proper keloid fibroblast and endothelial cell ratio

A higher proportion of endothelial cells gave a higher cell viability of keloid spheroids. Both A(F4E1) and A(F2E1) showed maintenance of compact spheroids with better cellular viability and propagation ability. However, only A(F4E1) showed significant increases in area. Accordingly, it was reasonable to think that the 4:1 ratio was the best ratio for evaluating and modeling keloids, followed by the 2:1 ratio.

Formation of keloid spheroids using patient-derived keloid fibroblasts and endothelial cells

We then generated keloid spheroids (K1, K2, K3) using patient-derived keloid fibroblasts obtained from biopsies at the same anatomical location from three patients. As 4:1 and 2:1 ratios were thought to be optimum ratios for keloid spheroids in previous experiments using commercially available ATCC keloid fibroblasts, we generated spheroids with patient-derived keloid fibroblasts and HUVECs at ratios of 4:1 (K1(F4E1), K2(F4E1), K3(F4E1)) and 2:1 (K1(F2E1), K2(F2E1), K3(F2E1)) (Fig. 4a, b).

On microscopy, K1 showed compact spheroids from day 3. However, these spheroids partially regressed on day 6. K2 and K3 formed compact spheroids from day 2. These spheroids were maintained until day 6. At day 6, the area of the spheroid ranged from 13,489 to 23,427 μm^2. The area was the largest in K3(F4E1) but the smallest in K2(F4E1).

Quantitative RT-PCR of keloid spheroids

RNA expression of each keloid spheroid was then compared with the same number of cells (fibroblasts and HUVECs) in 2D monolayer culture as control (Fig. 5). It was found that keloid spheroids had significantly increased expression levels of all keloid gene markers. When genetic markers were divided by the degree of average expression, *COL1A1*, *ADAM12*, and *HIF1A* showed less than a 10-fold increase. On the other hand, *COL3A1*, *HTRA1*, *TGFB1*, *TGFB3*, *CTHRC1*, and *MMP14* showed more than 10-fold increase. *COL1A1* and *TGFB3* showed more expression levels than *COL3A1* and *TGFB1*, respectively. When the effects of different cellular ratios on gene expression levels within each group were compared, gene expression levels were likely to increase when the cellular proportion of fibroblasts increased. This increase was statistically significant as determined by simple linear regression analysis in Supplementary Fig. S1 ($R^2 = 0.4$, $p < 0.001$). Since the 2:1 ratio showed the least increase among different ratios in all groups, the 2:1 ratio was not thought to be an optimum ratio for keloid spheroids as an in vitro model. Interestingly, keloid spheroids made of commercially available ATCC keloid fibroblasts showed higher gene expression levels than patient-derived keloid spheroids except for *ADAM12*. Patient-derived keloid spheroids demonstrated a different profile of gene expression in this analysis. This means that various clinical manifestations and activities of keloids can be reflected in patient-derived keloid spheroids.

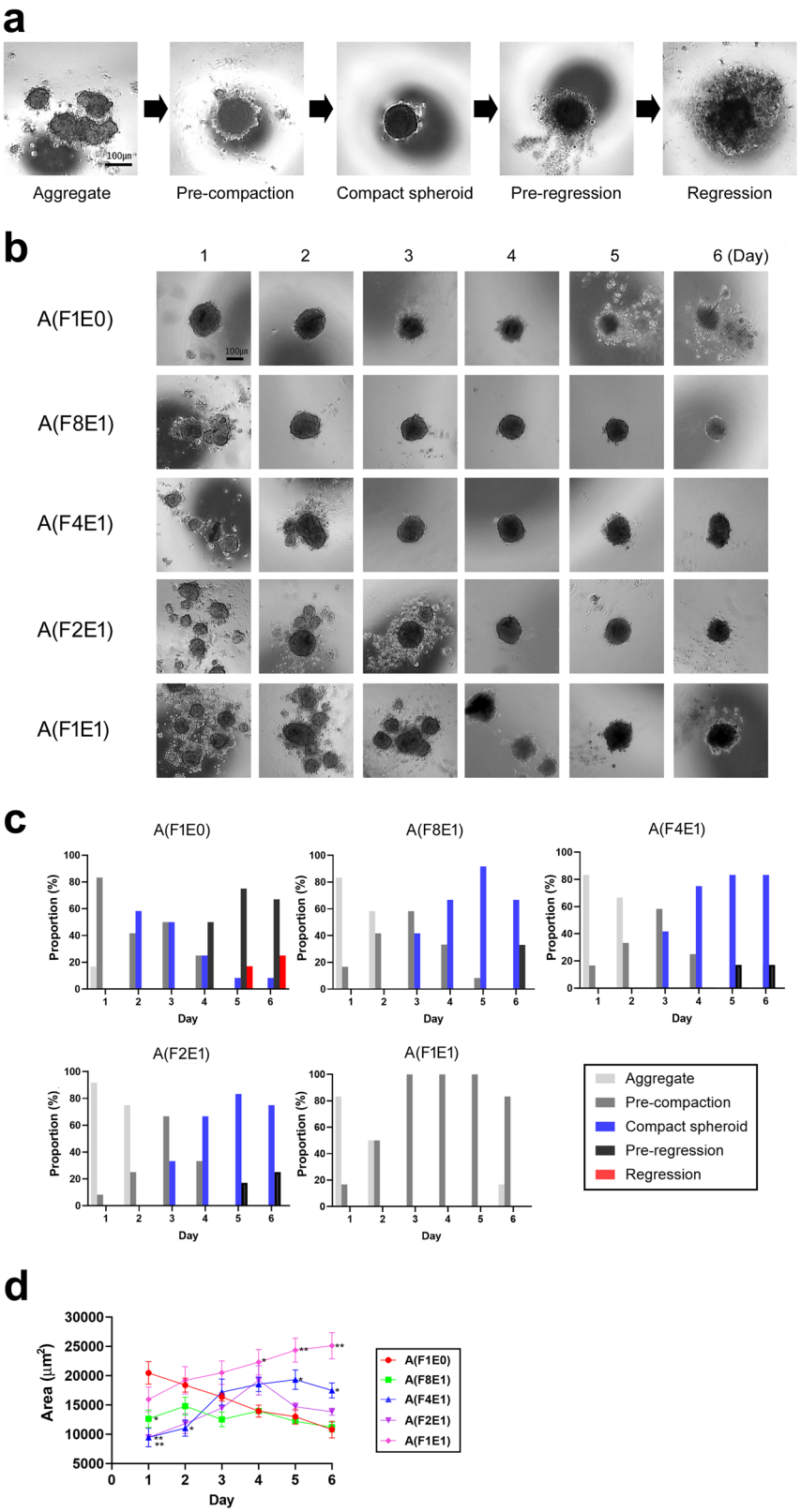

Fig. 1 | Formation of keloid spheroids using different ratios of ATCC keloid fibroblasts and HUVECs. a State change of aggregated cells according to density, scale bar = 100 μm. **b** Representative microscopic images of keloid spheroids at different cell ratios, scale bar = 200 μm. **c** Change of spheroid state on each day. Regression observed in A(F1E0) indicated that endothelial cells were necessary for maintaining keloid spheroids, whereas an excessively high ratio of endothelial cells in A(F1E1) prevented the formation of compact spheroids. **d** Changes of the spheroid area on each day. One-way ANOVA was performed to assess statistical significance. Data represent mean ± standard error of the mean of three biologically independent experiments. $*p < 0.05$ and $**p < 0.01$.

Drug assay

A drug assay was performed to assess the potential of keloid spheroids as an instrumental platform for in vitro drug screening. To minimize the effects of regression during drug assays, we examined the drug responses in keloid spheroids at the pre-compaction and compact spheroid stages. When combined with the results of spheroid size and cell viability, these findings suggest that day 4 spheroids are most suitable for drug assays. For comparison, drug assays were also conducted using 2D monolayer cultures of keloid fibroblasts, as well as spheroids and 2D monolayer cultures of normal fibroblasts. The drug responses of 3D spheroids, consisting of ATCC keloid fibroblasts and HUVECs at a 4:1 ratio (A(F4E1)), spheroids made with patient-derived keloid fibroblasts and HUVECs (K1(F4E1), K2(F4E1), K3(F4E1)), as well as spheroids made with normal fibroblasts and HUVECs at a 4:1 ratio (N(F4E1)), were evaluated. The drug responses in 2D

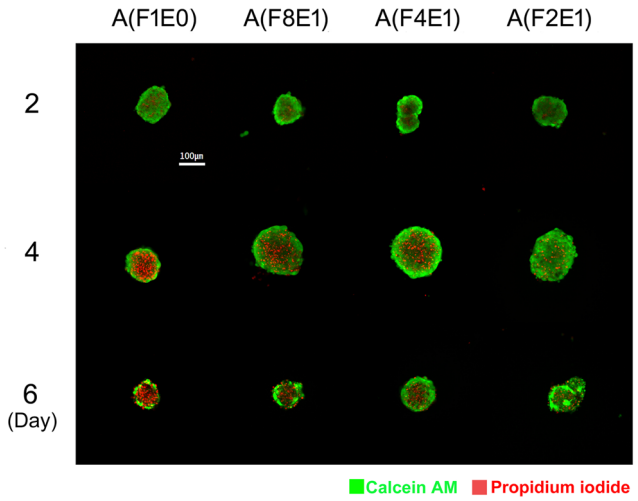

Fig. 2 | Cell viability assay of keloid spheroids using a live cell staining with calcein AM and a dead cell staining with propidium iodide. Viable cells are shown in green and nonviable cells are shown in red.

monolayer culture were evaluated using fibroblasts and HUVECs in the same cellular ratio as those used in each group of spheroids. Fig. 6 delineates both live/dead cell staining images of spheroids (Fig. 6, column a) and relative volumes of spheroids (Fig. 6, column b), as well as cell viability results from the 2D monolayer culture (Fig. 6, column c).

In 3D spheroids, the efficacy of administered drugs was deduced from notable alterations in diameter and a reduction in compactness as observed by confocal microscopy. It was further corroborated by a reduction in the relative volume of spheroids compared to the vehicle. It was observed that the drug responsivity exhibited by keloid spheroids depended on the source of fibroblasts. Notably, A(F4E1) manifested responsiveness to all tested drugs at concentrations of 10 μM and 100 μM (Fig. 6b, row A). In a contrasting observation, K1(F4E1) (Fig. 6b, row B) and K3(F4E1) (Fig. 6b, row D) exhibited a response solely to fluorouracil at a concentration of 100 μM, while demonstrating negligible responsiveness to both triamcinolone and bleomycin. Conversely, K2(F4E1) demonstrated susceptibility to fluorouracil at both 10 μM and 100 μM concentrations and exhibited tangible responses to triamcinolone and bleomycin at a concentration of 100 μM (Fig. 6b, row C). In normal fibroblast spheroids, drug responses were observed with fluorouracil at a concentration of 100 μM and bleomycin at both 10 μM and 100 μM (Fig. 6b, row E). For drug assays of 2D monolayer cultures, triamcinolone showed no effect across all groups (Fig. 6c).

Discussion

In recent years, not only tumor cells but also cells from the tumor environment including endothelial cells are used for the formation of heterogeneous spheroids[5,20–22]. These heterogeneous spheroids can represent in vivo tissues more than a 2D monolayer cell culture model. According to a previous study[4], heterogeneous spheroids with fibroblasts and macrophages show increased expression levels of genes related to fibrosis and inflammation with more collagen depositions than 2D monolayer culture. Another study has shown that gene expression profiles of heterogeneous spheroids with glioblastoma cells and HUVECs are consistent with in vivo glioblastoma studies[23].

In the present study, we generated keloid spheroids using commercially available keloid fibroblasts and patient-derived keloid fibroblasts with endothelial cells. Keloid fibroblasts were well mixed with endothelial cells in spheroids. Cells in the center of spheroids were found to have a short lifespan. However, the presence of endothelial cells could prolong the lifespan of central cells. Spheroids showed different degrees of aggregation, changes in area, and angiogenesis according to cellular ratio. Proper size and cellular ratio of spheroids are important factors for both the viability and representativeness of in vivo tissues. A previous study[4] has suggested that a diameter of 200 μm is an optimal diameter for spheroids due to increased viability, homogeneity, collagen deposits, and expression of fibrosis-related genes. All compact spheroids in this study had diameters of around 200 μm. For a proper cellular ratio, since there have been no studies mixing keloid fibroblasts and endothelial cells for keloid spheroids, we could only refer to former spheroid studies using normal fibroblasts and endothelial cells. One study has evaluated endothelial cell attachment, survival, and angiogenic activity in spheroids and suggested that the optimum cellular ratio for fibroblast and endothelial cells is 10:1[24]. Another study has confirmed that a vascular network is generated without needing artificial matrix compounds in spheroids with a 4:1 ratio of fibroblasts and endothelial cells[25]. In the present study, we found that a higher proportion of endothelial cells increased cell viability, while a higher proportion of fibroblasts increased gene expression. Before analyzing gene expression profiles, 4:1 and 2:1 ratios were thought to be optimum ratios for keloid spheroids. However, RT-PCR results for patient-derived keloid spheroids showed a dramatic increase in gene expression at a 4:1 ratio compared with those at a 2:1 ratio. Taken together, we propose that a 4:1 ratio is an optimum ratio for mixing keloid fibroblasts and endothelial cells for further keloid spheroids studies.

While former co-culture studies of keloid fibroblasts have shown increased vascular formation in endothelial cells[14,26], the role of endothelial cells in keloid spheroids has not been revealed yet. Keloid spheroids show a propagation ability essential for tumor survival. Interactions of fibroblasts and endothelial cells in keloids are increasingly emphasized by various multi-omics studies[15,17,27–30]. The role of vessels in keloids has also been widely studied in many clinical studies using different modalities[31–36]. Therefore, it is undeniable that endothelial cells are necessary for building keloid spheroids to represent in vivo keloids.

Vascular formations by endothelial cells are needed for cells to survive in either in vivo tissues or spheroid conditions. Although mixing endothelial cells could prolong the lifespan of spheroids to some degree, keloid spheroids still show many necrotic cells in the center. This phenomenon might be explained by the high metabolic rate of keloid fibroblasts and the role of hypoxia in the pathogenesis of keloids[37–41]. Based on these findings, keloid spheroids in this study might be an appropriate model for in vivo keloids. Nemosis, a programmed necrosis-like cell death of aggregated fibroblasts, might also explain this phenomenon[42]. One study[42] has suggested that fibroblasts in spheroids show activation with increased expression of genes associated with proinflammation, proteolysis, and growth factors. These spheroids are subsequently decomposed by a programmed necrosis-like cell death[42]. Since nemosis has not been identified in in vivo keloids yet, the role of nemosis in keloids should be identified through further studies.

Both commercial keloid fibroblast cell lines and patient-derived keloid fibroblasts were used to make keloid spheroids in this study. Keloid spheroids showed different compactness with different gene expression profiles and drug responses according to the fibroblasts used. The heterogeneity of keloids might be the reason for this. As shown in Fig. 5, spheroids generated with commercially available keloid fibroblast expressed higher levels of all keloid-associated genes (except for *ADAM12*) than patient-derived keloid spheroids. Commercially available keloid fibroblasts were assumed to have high keloid activities in every aspect. Therefore, they could not reflect individual patients' clinical conditions. In the present study, patient-derived keloid fibroblasts were all obtained from keloids in the chest to reduce possible bias of location. A previous study has insisted that the clinical condition of scars can be classified as collagen excess and vascular dominant status, in which a rather stable keloid is associated with the final result of collagen excess status, which indicates that an active keloid with unstoppable growth and discomfortable symptoms are more like to be related to a vascular dominant status[43].

We observed a significant elevation in the levels of keloid markers in a 3D spheroid model of keloids compared to a 2D culture model. These genetic markers were previously identified in our research on keloid patient samples as crucial indicators related to the pathogenesis of keloid formation[16]. *COL1A1* and *COL3A1* are essential components of the

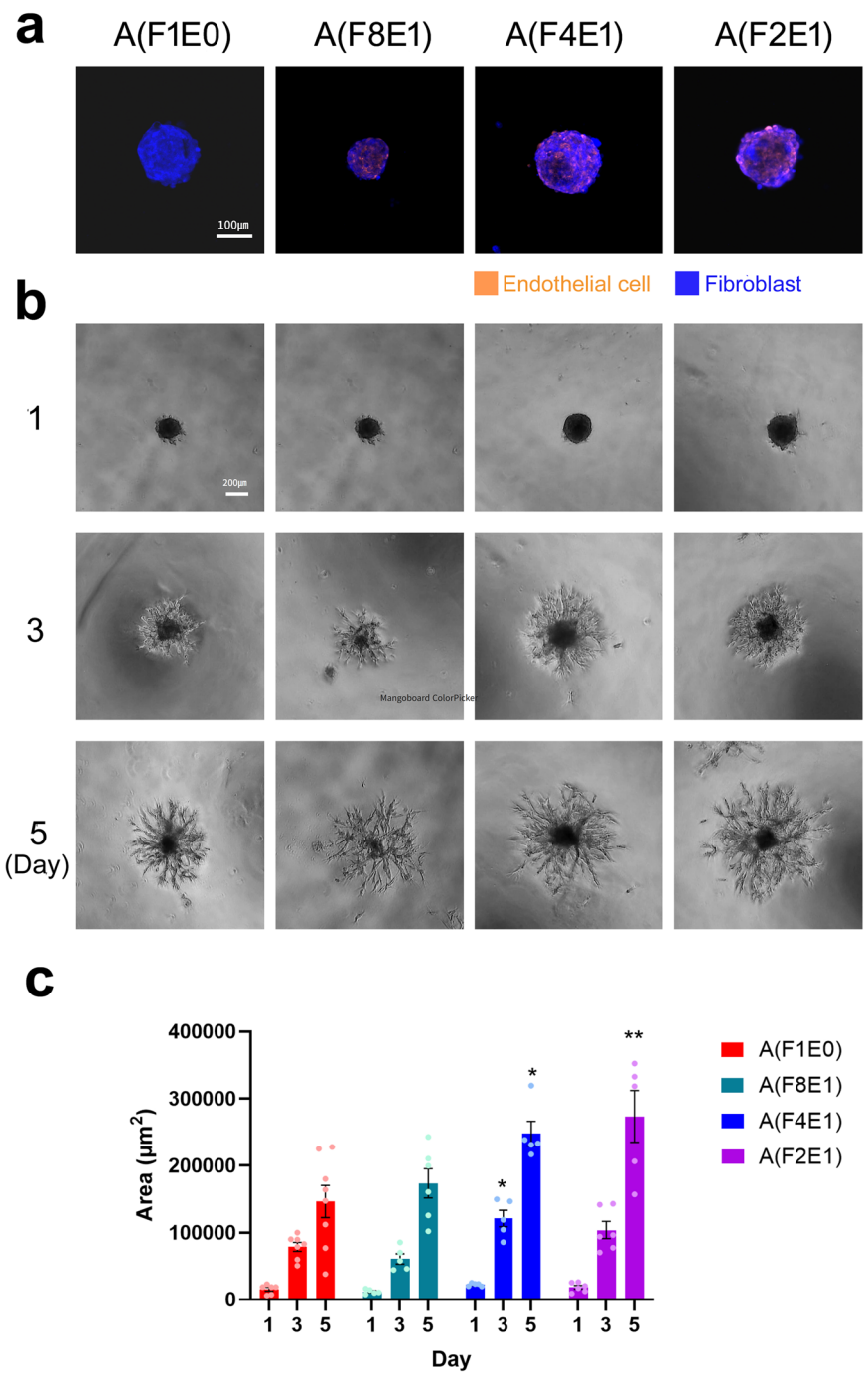

Fig. 3 | Composition and propagation assay of keloid spheroids. a Representative images of a mixture of fibroblasts and HUVECs in keloid spheroids on day 4, scale bar = 100 μm. **b** Representative images of propagation assay, scale bar = 200 μm. **c** Change of propagation area on each day. One-way analysis of variance was performed to assess statistical significance. Data represent mean ± standard error of the mean of at least five biologically independent replicates. $^{*}p < 0.05$ and $^{**}p < 0.01$.

extracellular matrix (ECM) and are typically upregulated in fibrotic conditions, contributing to the excessive collagen deposition characteristic of keloids. *TGFB1* and *TGFB3* are critical cytokines that modulate ECM production and fibroblast activity, potentially explaining their increased expression in the more physiologically relevant 3D environment. *HIF1A*, a key regulator of cellular responses to hypoxia, may be elevated due to the limited oxygen diffusion in the dense spheroid model, mimicking the hypoxic conditions of keloid tissue. *MMP14*, *HTRA1*, and *ADAM12* are involved in ECM remodeling and degradation, processes that are likely amplified in the 3D model where fibroblast and endothelial cell interactions are more complex and dynamic. *CTHRC1*, associated with tissue repair and remodeling, might be upregulated in response to the enhanced cell-cell interactions in the spheroid model. These findings suggest that the 3D spheroid model better replicates the in vivo environment of keloids, where fibroblast and endothelial cell interactions are more prominent, leading to the elevated expression of these genetic markers. Hypothetically, the 3D structure facilitates a more natural cell morphology and function, contributing to a better representation of keloid pathology and the associated molecular responses.

Spheroids have been extensively employed in drug screening, although the majority of research studies have focused on cancers[6,10,23]. Previous studies[44,45] have shown that 3D spheroids have more drug resistance than 2D culture models. This resistance arises because spheroids can mimic crucial in vivo tumor characteristics such as 3D morphology, hypoxia, and elevated genetic expressions[44,45]. In line with these findings, our study suggests that keloid spheroids likely offer a more accurate representation of in vivo keloids than 2D culture models, further highlighting the value of spheroids as in vitro models for drug screening. One study[46] has suggested that size-based analysis is an appropriate method for evaluating drug responses in tumor spheroids. Consequently, we assessed the volume of keloid spheroids to

evaluate drug responses. Depending on the type of cell utilized, keloid spheroids exhibited varying drug responses in terms of volume reduction, which might provide insights into the in vivo treatment response in keloid patients. This study demonstrated that commercially available keloid fibroblasts derived spheroid responded well to triamcinolone, fluorouracil, and bleomycin, while spheroid made of patient-derived fibroblasts showed different responses to three drugs. Interesting findings were that spheroids from patients-derived fibroblasts did not respond well to triamcinolone,

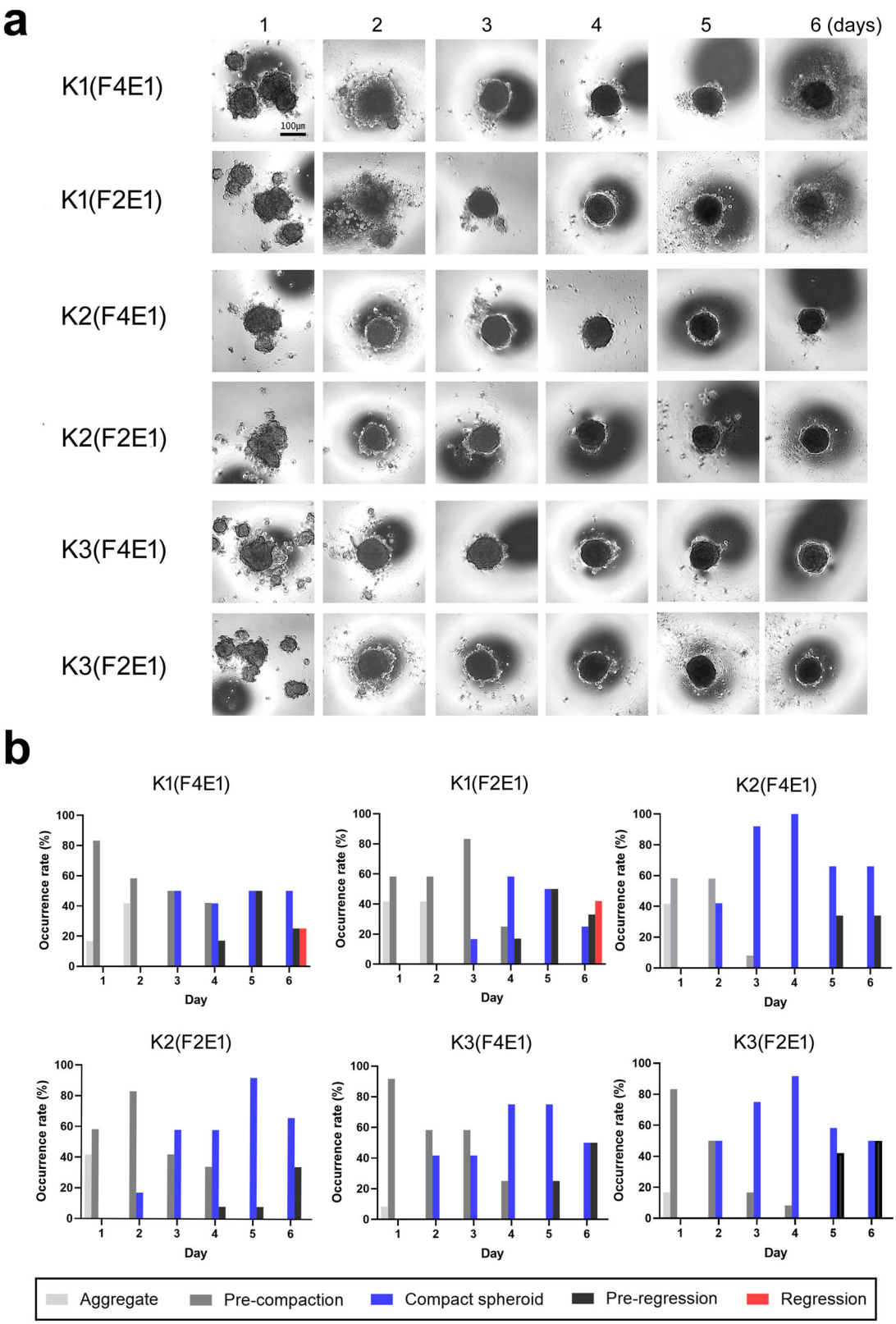

Fig. 4 | Formation of keloid spheroids using patient-derived keloid fibroblasts and HUVECs at different cellular ratios. a Representative microscopic images of keloid spheroids of K1, K2, and K3 with different cell ratios, scale bar = 200 μm. **b** Change of spheroid state on each day. Depending on the cell source, regression was only observed in K1, whereas compact spheroids were well-maintained in both K2 and K3.

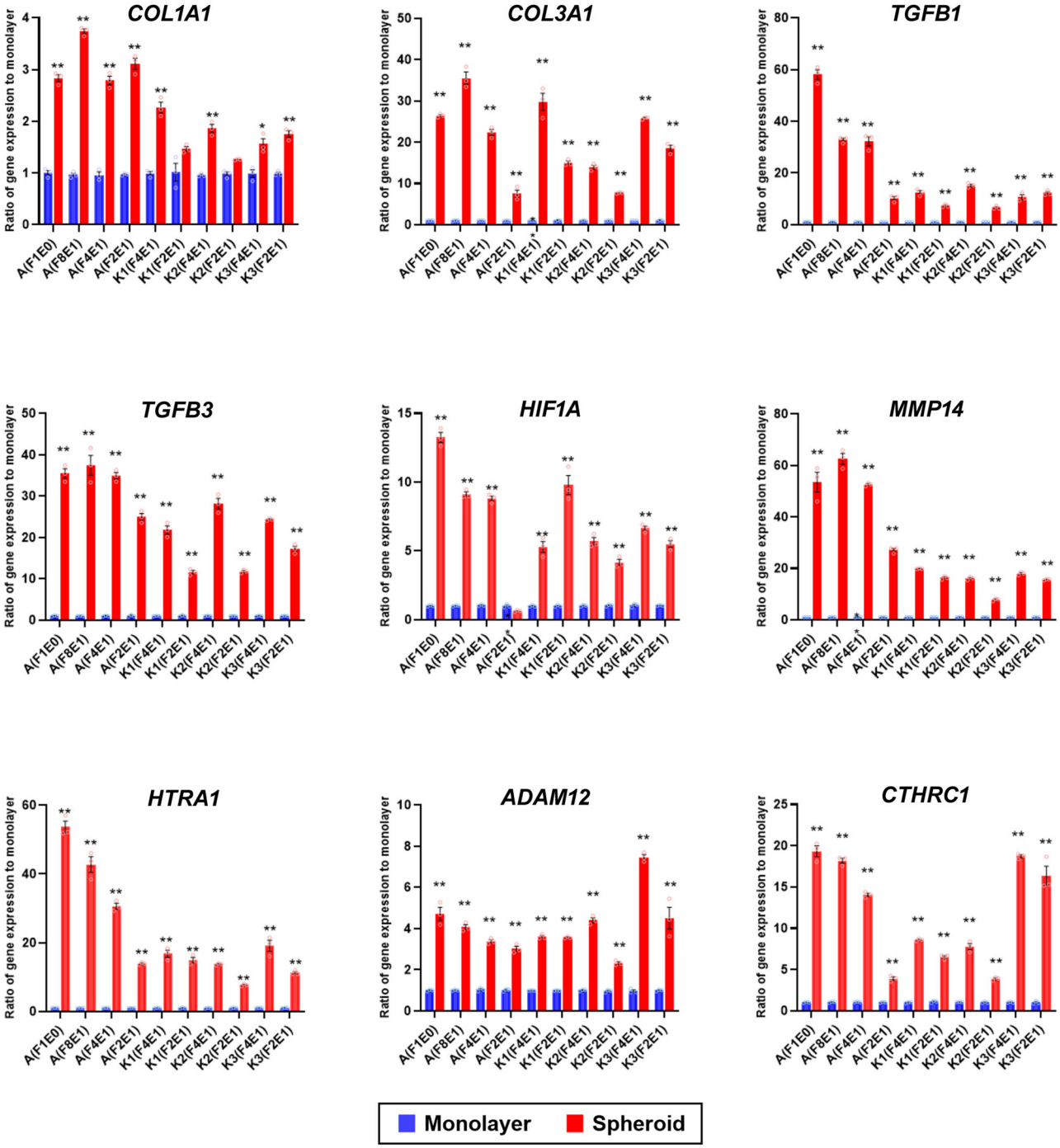

Fig. 5 | Quantification with real-time PCR. Relative RNA expression levels in each spheroid group compared to those in 2D monolayer cultured fibroblasts and HUVECs at day 4. One-way analysis of variance was performed to assess statistical significance. Data represent mean ± standard error of the mean of biological triplicate samples. $^{*}p < 0.05$ and $^{**}p < 0.01$.

which is the first-line drug for the treatment of keloid. In practice, patients who donated keloid fibroblasts (K1, K2, and K3) would not respond well to triamcinolone intralesional injection, and combined with these results, patient-derived keloid spheroids might be more suitable for personalized medicine. The potential role of keloid spheroids for predicting treatment responses for precision medicine or developing new drugs is promising.

A limitation of this study was that HUVECs were used to generate keloid spheroid. Multi-omics studies have shown that keloid-specific endothelial cell clusters can express different genetic patterns[16,17,47]. If we separate and use endothelial cells from keloid tissues, they could reflect better in vivo keloid microenvironments. The low cellular viability in the center of keloid spheroids was another limitation of this study. Although this might be explained by hypoxia in keloids or nemosis of fibroblast spheroids as mentioned above, methods to increase the cell viability of spheroids are needed. Adding growth factors or collagen fibrils in spheroids might prolong cell viability[48,49]. Further studies are needed to find ways to prolong the lifespan of spheroids.

In this study, we developed a 3D keloid spheroid model using a combination of keloid fibroblasts and endothelial cells, which better represents the complex cellular interactions and gene expression profiles observed in vivo compared to traditional 2D cultures. The optimal cellular ratio of fibroblasts to endothelial cells was identified as 4:1, which effectively

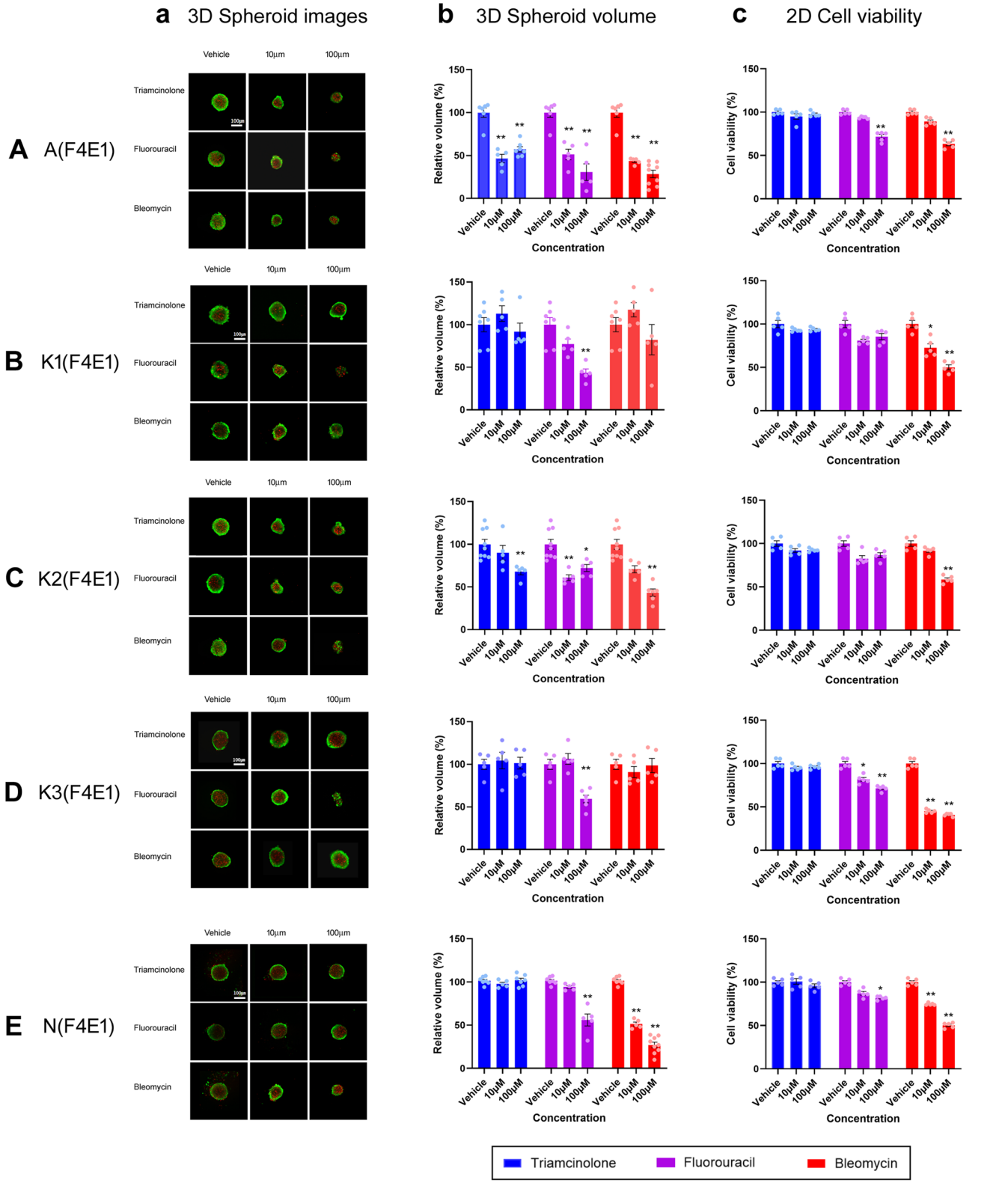

Fig. 6 | Drug responses in keloid and normal fibroblast spheroids and 2D monolayer cultures. a 3D spheroid images: Representative images of spheroids made from different cell sources treated with vehicle, 10 μM, and 100 μM concentrations of triamcinolone, fluorouracil, and bleomycin. Calcein AM (green) was used for live cell staining and propidium iodide (red) for dead cell staining. Scale bar = 100 μm. **b** 3D spheroid volume: Changes in the relative volume of spheroids for each drug and concentration. Drug efficacy in 3D spheroids was determined by changes in spheroid diameter and compactness observed via confocal microscopy and quantified by relative spheroid volume reduction. **c** 2D cell viability: Cell viability results from the 2D monolayer culture for each drug and concentration. Rows A, B, C, D, and E correspond to different cell sources: A(F4E1) (ATCC keloid fibroblasts), K1(F4E1), K2(F4E1), K3(F4E1) (patient-derived keloid fibroblasts), and N(F4E1) (normal fibroblasts), respectively. One-way ANOVA was performed to assess statistical significance. Data represent mean ± standard error of the mean of at least five biologically independent replicates. $^{*}p < 0.05$, $^{**}p < 0.01$.

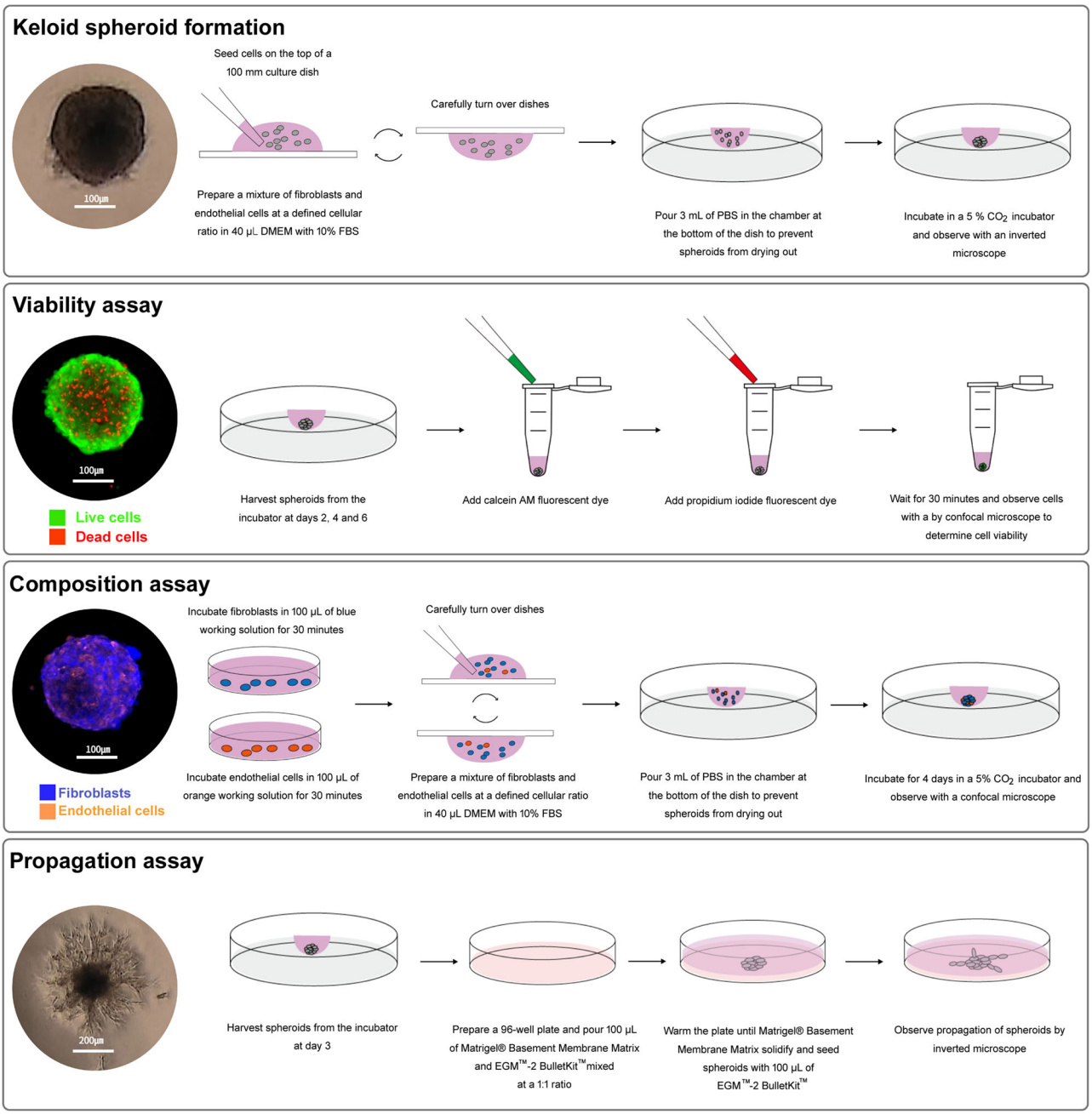

Fig. 7 | Detailed methods of keloid spheroids formation, viability assay, composition assay, and propagation assay.

balances the viability and activity of keloid spheroids, highlighting the crucial role of endothelial cells in keloid spheroids. The study also highlighted the heterogeneity in drug responses among keloid spheroids, underscoring the potential of this model for personalized medicine. The differential drug responses observed in these spheroids suggest that keloid spheroids could be instrumental in predicting individual patient responses and guiding personalized treatment strategies, ultimately improving clinical outcomes for keloid patients.

Methods

Detailed methods are described in Fig. 7.

Preparation of fibroblasts and endothelial cells

Keloid fibroblasts were obtained from a commercial cell line and keloid patients who were confirmed to have keloids based on clinical features and histopathologic examination. This study was approved by the Institutional Review Board (IRB) of Samsung Medical Center (IRB number: SMC 2020-03-032). An informed consent was obtained from all patients. All ethical regulations relevant to human research participants were followed. For group A, a commercial keloid fibroblast cell line (CRL1762, ATCC, Manassas, VA, USA) was used. For groups K1, K2, and K3, keloid fibroblasts were derived from patients who had different clinical responses to treatment, all obtained from the same anatomical location via excisional biopsies (Supplementary Table 1). For group N, normal fibroblasts were obtained from the skin of a healthy individual without keloids for comparison in the drug assay.

Keloid tissues were planted onto dishes for an explant culture and fibroblasts were separated. Fibroblasts were cultured in DMEM (Thermo Fisher Scientific, Waltham, MA, USA) supplemented with 10% heat-inactivated fetal bovine serum (Thermo Fisher Scientific, Waltham, MA, USA), and 1% penicillin-streptomycin (Gibco, Carlsbad, CA, USA). For endothelial cells, a commercial cell line of human umbilical vein endothelial

cells (HUVECs) (C2519A, Lonza, Basel, Switzerland) was used and cultured in EGM™-2 BulletKit™ media (Lonza, Basel, Switzerland). Fibroblasts and HUVECs used for all experiments were between passages 3 and 5.

Spheroid formation

The number of fibroblasts per spheroid was fixed to be 2000. For endothelial cells, the number of cells was changed to 0, 250, 500, 1000, and 2000 to find the optimal cellular ratio for keloid spheroids. Fibroblasts and endothelial cells were then mixed according to the defined cellular ratio (1:0, 8:1, 4:1, 2:1, 1:1). They were loaded on the top of a 100 mm culture dish. The two types of cells were mixed in 40 μL DMEM supplemented with 10% heat-inactivated fetal bovine serum (Thermo Fisher Scientific, Waltham, MA, USA), and 1% penicillin-streptomycin (Gibco, Carlsbad, CA, USA). A hanging drop method was used to generate spheroids. Dishes were carefully turned over and 3 mL of PBS was placed in the chamber at the bottom of the dish to prevent spheroids from drying out. They were then incubated in a 5% CO2 incubator. Their daily state was observed using an inverted microscope (CKX53, Olympus, Shinjuku, Japan). The area of the spheroid was measured from the darkest area in the microscopic images. The experiments were repeated three times independently. For each independent experiment, quantification was performed on at least 8 spheroids per culture condition and per cell line.

Cell viability assay

Spheroids were collected from the incubator on days 2, 4, and 6. A Live/Dead Cell Double Staining Kit (Sigma-Aldrich, Burlington, MA, USA) was used to determine the cell viability of spheroids. Spheroids were stained according to the manufacturer's protocol. Live cells were observed at an excitation wavelength of 490 nm of green fluorescent dye calcein AM and dead cells were observed at an excitation wavelength of 545 nm of propidium iodide fluorescent dye using a confocal laser scanning microscope (LSM800, Carl Zeiss, Oberkochen, Germany). The experiments were repeated three times independently. For each independent experiment, at least 5 spheroids were prepared per culture condition and per cell line.

Composition assay

Fibroblasts were incubated with 100 μL of 1× Track It™ Blue working solution (AAT Bioquest, Pleasanton, CA, USA) in 100 mm culture dishes for 30 min using a Cell Explorer™ Live Cell Tracking Kit (AAT Bioquest, Pleasanton, CA, USA). Endothelial cells were incubated with 100 μL of 1× Track It™ Orange working solution (AAT Bioquest, Pleasanton, CA, USA) in a 100 mm culture dish for 30 min using a Cell Explorer™ Live Cell Tracking Kit (AAT Bioquest, Pleasanton, CA, USA). Next, fluorescent dye was washed. Fibroblasts and endothelial cells were then mixed at a predefined cellular ratio to make spheroids. After the incubation period, blue fluorescence was observed using a 450/40 nm filter, and orange fluorescence was observed using a 575/26 nm filter of a confocal laser scanning microscope (LSM800, Carl Zeiss, Oberkochen, Germany). The experiments were repeated three times independently. For each independent experiment, at least 5 spheroids were prepared per culture condition and per cell line.

Propagation assay

Spheroids incubated for 3 days were used for propagation assay. EGM™-2 BulletKit™ medium (Lonza, Basel, Switzerland) and Matrigel® Basement Membrane Matrix (Corning, Corning, NY, USA) were mixed at a 1:1 ratio and a 100 μL per well of the mixture was loaded into a 96-well culture plate. Spheroids were then put on the plate and incubated. After incubation for 1, 3, and 5 days, images were taken using an inverted microscope (CKX53, Olympus, Shinjuku, Tokyo, Japan) and quantified using ImageJ (National Institutes of Health, Bethesda, MD, USA). The experiments were repeated three times independently. For each independent experiment, quantification was performed on at least 5 spheroids per culture condition and per cell line.

Quantification using RT-PCR

Spheroids were incubated for three days and subjected to gene expression analysis by quantitative RT-PCR. A total of 70 spheroids for each group were used. The same amounts of fibroblasts and endothelial cells in each spheroid were cultured using 2D monolayer culture to compare gene expression profiles. The experiments were repeated three times independently. All samples were run in triplicate. Representative genetic markers associated with keloid pathogenesis were analyzed by referring to previous keloid studies on *COL1A1*, *COL3A1*, *TGFB1*, *TGFB3*, *HIF1A*, *MMP14*, *HTRA1*, *ADAM12*, and *CTHRC1*[16,40,50–52]. Total RNAs were extracted using an RNeasy mini kit (Qiagen, Hilden, Germany). Template cDNAs were obtained by reverse transcription of total RNAs using oligo (dT) primer and a PrimeScript™ RT reagent Kit (Takara, Tokyo, Japan). PCR amplification was carried out using SYBR® Green Realtime PCR Master Mix (Toyobo, Osaka, Japan). A normalization of the RNA level was performed against the *ACTB* gene. Primers used for real-time RT-PCR are listed in Supplementary Table 2.

Drug assay

Triamcinolone, fluorouracil, and bleomycin, the three most commonly used drugs for keloids in clinical settings, were selected for drug assay. Drug compounds were obtained from Selleckchem (Houston, TX, USA). Each drug was dissolved in DMSO at concentrations of 10 μM and 100 μM, respectively. Drug assays were conducted on both spheroids and 2D monolayer cultures, with responses in normal fibroblasts from a healthy individual also evaluated for comparison.

For the drug assays of spheroids, the spheroids were prepared and maintained in culture for 2 days prior to treatment. On day 2, spheroids were collected from the incubator and treated with drug compounds for 48 h. Spheroids were visually evaluated using a Live/Dead Cell Double Staining Kit (Sigma-Aldrich, Burlington, MA, USA) on a confocal laser scanning microscope (LSM800, Carl Zeiss, Oberkochen, Germany) to observe relative fluorescence levels associated with concentrations of each drug. The diameter of each spheroid was measured using ImageJ (National Institutes of Health, Bethesda, MD, USA) and the volume was calculated assuming a spherical shape. The relative volume of spheroids was determined using vehicles as reference (100%). The experiments were repeated three times independently. For each independent experiment, quantification was performed on at least 5 spheroids per culture condition and per cell line.

For the 2D viability measurement, fibroblasts and endothelial cells at the same cellular ratio as in the spheroids were seeded into 100 μL of DMEM growth media per well in a 96-well plate, with a total of 1500 cells per well, and incubated for 24 h. Three types of drugs were administered at varying concentrations. After 48 h of incubation, 10 μL of Cell Counting Kit-8 (Dojindo, Kumamoto, Japan) was added per well. Optical density was measured and quantified 1 h later using a multimode microplate reader (LB940, Berthold Technologies, Bad Wildbad, Germany). The experiments were repeated three times independently. For each independent experiment, quantification was performed on at least 5 wells per culture condition and per cell line.

Statistics and reproducibility

All statistical analyses were performed using Prism 9.3.1 (GraphPad, San Diego, CA, USA). The size of spheroids, propagation area, RT-PCR gene expression levels, and 3D spheroid volume and 2D cell viability in the drug assay were compared using one-way analysis of variance (ANOVA). The descriptions related to the statistics for each experiment are provided in the corresponding sections of the "Methods" section. In the RT-PCR analysis, statistical results demonstrating that an increase in the proportion of fibroblasts in spheroids correlates with elevated keloid gene expression levels were analyzed using simple linear regression. The criterion for statistical significance was set at $p < 0.05$.

Reporting summary

Further information on research design is available in the Nature Portfolio Reporting Summary linked to this article.

Data availability

All data supporting the findings of this study are available within the paper and its Supplementary Information. The source data behind the graphs in the paper can be found in Supplementary Data 1.

Abbreviations

2D	two-dimensional
3D	three-dimensional
A	keloid spheroids generated using ATCC keloid fibroblasts
E	cellular ratio of endothelial cells
F	cellular ratio of fibroblasts
HUVECs	human umbilical vein endothelial cells
K	keloid spheroids generated using patient-derived keloid fibroblasts

Received: 23 January 2024; Accepted: 1 November 2024;
Published online: 08 November 2024

References

1. Ud-Din, S. & Bayat, A. Non-animal models of wound healing in cutaneous repair: in silico, in vitro, ex vivo, and in vivo models of wounds and scars in human skin. *Wound Repair Regen.* **25**, 164–176 (2017).
2. Limandjaja, G. C., Niessen, F. B., Scheper, R. J. & Gibbs, S. The keloid disorder: heterogeneity, histopathology, mechanisms and models. *Front. Cell. Dev. Biol.* **8**, 360 (2020).
3. Lebeko, M., Khumalo, N. P. & Bayat, A. Multi-dimensional models for functional testing of keloid scars: in silico, in vitro, organoid, organotypic, ex vivo organ culture, and in vivo models. *Wound Repair Regen.* **27**, 298–308 (2019).
4. Tan, Y. et al. Human fibroblast-macrophage tissue spheroids demonstrate ratio-dependent fibrotic activity for in vitro fibrogenesis model development. *Biomater. Sci.* **8**, 1951–1960 (2020).
5. Franchi-Mendes, T., Eduardo, R., Domenici, G. & Brito, C. 3D cancer models: depicting cellular crosstalk within the tumour microenvironment. *Cancers***13**, 4610 (2021).
6. Khaitan, D. & Dwarakanath, B. S. Multicellular spheroids as an in vitro model in experimental oncology: applications in translational medicine. *Expert. Opin. Drug Discov.* **1**, 663–675 (2006).
7. Fennema, E., Rivron, N., Rouwkema, J., van Blitterswijk, C. & de Boer, J. Spheroid culture as a tool for creating 3D complex tissues. *Trends Biotechnol.* **31**, 108–115 (2013).
8. Lin, R. Z. & Chang, H. Y. Recent advances in three-dimensional multicellular spheroid culture for biomedical research. *Biotechnol. J.* **3**, 1172–1184 (2008).
9. Kunz-Schughart, L. A., Kreutz, M. & Knuechel, R. Multicellular spheroids: a three-dimensional in vitro culture system to study tumour biology. *Int J. Exp. Pathol.* **79**, 1–23 (1998).
10. Song, Y. et al. Patient-derived multicellular tumor spheroids towards optimized treatment for patients with hepatocellular carcinoma. *J. Exp. Clin. Cancer Res.* **37**, 109 (2018).
11. Lee, W. J., Choi, I. K., Lee, J. H., Kim, Y. O. & Yun, C. O. A novel three-dimensional model system for keloid study: organotypic multicellular scar model. *Wound Repair Regen.* **21**, 155–165 (2013).
12. Sato, M., Ishikawa, O. & Miyachi, Y. Distinct patterns of collagen gene expression are seen in normal and keloid fibroblasts grown in three-dimensional culture. *Br. J. Dermatol.* **138**, 938–943 (1998).
13. Hahn, J. M. et al. Keloid-derived keratinocytes exhibit an abnormal gene expression profile consistent with a distinct causal role in keloid pathology. *Wound Repair Regen.* **21**, 530–544 (2013).
14. Ong, C. T. et al. Epithelial-mesenchymal interactions in keloid pathogenesis modulate vascular endothelial growth factor expression and secretion. *J. Pathol.* **211**, 95–108 (2007).
15. Ogawa, R. & Akaishi, S. Endothelial dysfunction may play a key role in keloid and hypertrophic scar pathogenesis - keloids and hypertrophic scars may be vascular disorders. *Med. Hypotheses* **96**, 51–60 (2016).
16. Shim, J. et al. Integrated analysis of single-cell and spatial transcriptomics in keloids: highlights on fibrovascular interactions in keloid pathogenesis. *J. Invest. Dermatol.* **142**, 2128–2139.e11 (2022).
17. Liu, X. et al. Single-cell RNA-sequencing reveals lineage-specific regulatory changes of fibroblasts and vascular endothelial cells in keloids. *J. Invest. Dermatol.* **142**, 124–135.e11 (2022).
18. Dirand, Z., Tissot, M., Chatelain, B., Viennet, C. & Rolin, G. Is spheroid a relevant model to address fibrogenesis in keloid research? *Biomedicines* **11**, 2350 (2023).
19. Granato, G. et al. Generation and analysis of spheroids from human primary skin myofibroblasts: an experimental system to study myofibroblasts deactivation. *Cell Death Discov.* **3**, 17038 (2017).
20. Lazzari, G. et al. Multicellular spheroid based on a triple co-culture: A novel 3D model to mimic pancreatic tumor complexity. *Acta Biomater.* **78**, 296–307 (2018).
21. Franchi-Mendes, T., Lopes, N. & Brito, C. Heterotypic tumor spheroids in agitation-based cultures: a scaffold-free cell model that sustains long-term survival of endothelial cells. *Front. Bioeng. Biotechnol.* **9**, 649949 (2021).
22. Dorst, N., Oberringer, M., Grasser, U., Pohlemann, T. & Metzger, W. Analysis of cellular composition of co-culture spheroids. *Ann. Anat.* **196**, 303–311 (2014).
23. Avci, N. G., Fan, Y., Dragomir, A., Akay, Y. M. & Akay, M. Investigating the influence of HUVECs in the formation of glioblastoma spheroids in high-throughput three-dimensional microwells. *IEEE Trans. Nanobiosci.* **14**, 790–796 (2015).
24. Kunz-Schughart, L. A. et al. Potential of fibroblasts to regulate the formation of three-dimensional vessel-like structures from endothelial cells in vitro. *Am. J. Physiol. Cell Physiol.* **290**, C1385–C1398 (2006).
25. Eckermann, C. W., Lehle, K., Schmid, S. A., Wheatley, D. N. & Kunz-Schughart, L. A. Characterization and modulation of fibroblast/endothelial cell co-cultures for the in vitro preformation of three-dimensional tubular networks. *Cell Biol. Int.* **35**, 1097–1110 (2011).
26. Syed, F. & Bayat, A. Notch signaling pathway in keloid disease: enhanced fibroblast activity in a Jagged-1 peptide-dependent manner in lesional vs. extralesional fibroblasts. *Wound Repair Regen.* **20**, 688–706 (2012).
27. Zheng, W., Lin, G. & Wang, Z. Bioinformatics study on different gene expression profiles of fibroblasts and vascular endothelial cells in keloids. *Medicine* **100**, e27777 (2021).
28. Karasek, M. A. Does transformation of microvascular endothelial cells into myofibroblasts play a key role in the etiology and pathology of fibrotic disease? *Med. Hypotheses* **68**, 650–655 (2007).
29. Kiya, K. et al. Endothelial cell-derived endothelin-1 is involved in abnormal scar formation by dermal fibroblasts through RhoA/Rho-kinase pathway. *Exp. Dermatol.* **26**, 705–712 (2017).
30. Noishiki, C., Takagi, G., Kubota, Y. & Ogawa, R. Endothelial dysfunction may promote keloid growth. *Wound Repair Regen.* **25**, 976–983 (2017).
31. Eura, S. et al. Hemodynamics and vascular histology of keloid tissues and anatomy of nearby blood vessels. *Plast. Reconstr. Surg. Glob. Open* **10**, e4374 (2022).
32. Sugimoto, A., Ono, S., Usami, S., Nitta, T. & Ogawa, R. Older patients and patients with severe arteriosclerosis are less likely to develop keloids and hypertrophic scars after thoracic midline incision: a survey-based analysis of 328 cases. *Plast. Reconstr. Surg.* **150**, 659–669 (2022).
33. Demir, T., Takada, H., Furuya, K., Sokabe, M. & Ogawa, R. Role of skin stretch on local vascular permeability in murine and cell culture models. *Plast. Reconstr. Surg. Glob. Open* **10**, e4084 (2022).

34. Chen, C. et al. Activity of keloids evaluated by multimodal photoacoustic/ultrasonic imaging system. *Photoacoustics* **24**, 100302 (2021).
35. Lobos, N., Wortsman, X., Valenzuela, F. & Alonso, F. Color Doppler ultrasound assessment of activity in keloids. *Dermatol. Surg.* **43**, 817–825 (2017).
36. Yoo, M. G. & Kim, I. H. Keloids and hypertrophic scars: characteristic vascular structures visualized by using dermoscopy. *Ann. Dermatol.* **26**, 603–609 (2014).
37. Vincent, A. S. et al. Human skin keloid fibroblasts display bioenergetics of cancer cells. *J. Invest. Dermatol.* **128**, 702–709 (2008).
38. Su, Z. et al. Warburg effect in keloids: a unique feature different from other types of scars. *Burns* **48**, 176–183 (2022).
39. Lei, R. et al. HIF-1alpha promotes the keloid development through the activation of TGF-beta/Smad and TLR4/MyD88/NF-kappaB pathways. *Cell Cycle* **18**, 3239–3250 (2019).
40. Kang, Y. et al. Hypoxia and HIF-1alpha regulate collagen production in keloids. *J. Invest. Dermatol.* **140**, 2157–2165 (2020).
41. Jusman, S. W. A., Sari, D. H., Ningsih, S. S., Hardiany, N. S. & Sadikin, M. Role of hypoxia inducible factor-1 alpha (HIF-1alpha) in cytoglobin expression and fibroblast proliferation of keloids. *Kobe J. Med. Sci.* **65**, E10–E18 (2019).
42. Vaheri, A., Enzerink, A., Rasanen, K. & Salmenpera, P. Nemosis, a novel way of fibroblast activation, in inflammation and cancer. *Exp. Cell Res.* **315**, 1633–1638 (2009).
43. Yuan, B., Upton, Z., Leavesley, D., Fan, C. & Wang, X. Q. Vascular and collagen target: a rational approach to hypertrophic scar management. *Adv. Wound Care* **12**, 38–55 (2023).
44. Swierczewska, M. et al. The response and resistance to drugs in ovarian cancer cell lines in 2D monolayers and 3D spheroids. *Biomed. Pharmacother.* **165**, 115152 (2023).
45. Imamura, Y. et al. Comparison of 2D- and 3D-culture models as drug-testing platforms in breast cancer. *Oncol. Rep.* **33**, 1837–1843 (2015).
46. Thakuri, P. S., Gupta, M., Plaster, M. & Tavana, H. Quantitative size-based analysis of tumor spheroids and responses to therapeutics. *Assay Drug Dev. Technol.* **17**, 140–149 (2019).
47. Matsumoto, N. M. et al. Gene expression profile of isolated dermal vascular endothelial cells in keloids. *Front. Cell. Dev. Biol.* **8**, 658 (2020).
48. Son, J., Tae, J. Y., Min, S. K., Ko, Y. & Park, J. B. Fibroblast growth factor-4 maintains cellular viability while enhancing osteogenic differentiation of stem cell spheroids in part by regulating RUNX2 and BGLAP expression. *Exp. Ther. Med.* **20**, 2013–2020 (2020).
49. Kuo, C. T. et al. Three-dimensional spheroid culture targeting versatile tissue bioassays using a PDMS-based hanging drop array. *Sci. Rep.* **7**, 4363 (2017).
50. Yamawaki, S. et al. HtrA1 is specifically up-regulated in active keloid lesions and stimulates keloid development. *Int. J. Mol. Sci.* **19**, 1275 (2018).
51. Zhao, M. J. et al. Increased Cthrc1 activates normal fibroblasts and suppresses keloid fibroblasts by inhibiting TGF-beta/Smad signal pathway and modulating YAP subcellular location. *Curr. Med. Sci.* **38**, 894–902 (2018).
52. Seifert, O. et al. Identification of unique gene expression patterns within different lesional sites of keloids. *Wound Repair Regen.* **16**, 254–265 (2008).

Acknowledgements

This work was supported by the National Research Foundation of Korea (NRF) grant funded by the Korea government (MSIT) (RS-2024-00345769). The study was supported by the Health Fellowship Foundation (2023). This research was supported by a grant of the MD-Phd/Medical Scientist Training Program through the Korea Health Industry Development Institute (KHIDI), funded by the Ministry of Health & Welfare, Republic of Korea.

Author contributions

Y.C., H-S.J., and J.H.L. designed the study. Y.C., H-S.J., E.Y., and M-H.K. conducted the experiments. Y.C., H-S.J., J.S., H.N., and S.O. analyzed the data. Y.C., J-H.P., D.L., and J.H.L. drafted and revised the manuscript. All authors read and approved the final version of the manuscript.

Competing interests

The authors declare no competing interests.

Additional information

Supplementary information The online version contains supplementary material available at https://doi.org/10.1038/s42003-024-07194-2.

Correspondence and requests for materials should be addressed to Jong Hee Lee.

Peer review information *Communications Biology* thanks Gwenaël Rolin and the other, anonymous, reviewer for their contribution to the peer review of this work. Primary Handling Editor: Ophelia Bu.